

Density functional calculations of Ge(105): Local basis sets and $O(N)$ methods

T. Miyazaki,^{1,*} D. R. Bowler,^{2,3,4,†} R. Choudhury,^{4,‡} and M. J. Gillan^{2,3,4,§}

¹National Institute for Materials Science, 1-2-1 Sengen, Tsukuba, Ibaraki 305-0047, Japan

²Materials Simulation Laboratory, University College London, Gower Street, London WC1E 6BT, United Kingdom

³London Centre for Nanotechnology, University College London, 17-19 Gordon Street, London WC1H 0AH, United Kingdom

⁴Department of Physics and Astronomy, University College London, Gower Street, London WC1E 6BT, United Kingdom

(Received 15 March 2007; revised manuscript received 6 July 2007; published 21 September 2007)

The Ge(105) surface has attracted attention recently, both from interest in the reconstruction itself and because the facets of three-dimensional hut clusters which form during heteroepitaxy of Ge on Si(001) are strained Ge(105) surfaces. We present density functional theory (DFT) studies of this surface using local basis sets as a preparation for $O(N)$ DFT studies of full hut clusters on Si(001). Two aspects have been addressed. First, the detailed buckling structure of the dimers forming the surface reconstruction is modeled using DFT and tight binding; two different structures are found to be close in stability, the second of which may be important in building hut-cluster facets [as opposed to perfect Ge(105) surfaces]. Second, the accuracy that can be achieved using local basis sets for DFT calculations is investigated, with $O(N)$ calculations as the target. Two different basis sets are considered: B splines, also known as blips, and pseudoatomic orbitals; B splines are shown to reproduce the result of plane-wave calculations extremely accurately. The accuracy of different modes of calculation (from non-self-consistent *ab initio* tight binding to full DFT) is investigated, along with the effect of cutoff radius for $O(N)$ operations. These results all show that accurate, linear-scaling DFT calculations are possible for this system and give quantitative information about the errors introduced by different localization criteria.

DOI: [10.1103/PhysRevB.76.115327](https://doi.org/10.1103/PhysRevB.76.115327)

PACS number(s): 68.35.Md, 71.15.Ap, 61.46.-w, 68.03.Hj

I. INTRODUCTION

Vicinal semiconductor surfaces have been the subject of numerous investigations recently, because of their reconstructions, step structures, and other nanoscale structure.¹ The Ge(105) surface, in particular, is important because of its major role in the energetics of the self-assembled nanostructures known as “hut clusters” that are formed when Ge is epitaxially deposited on the Si(001) surface.² However, despite this importance, the exact details of the reconstruction are still under investigation. While there is good experimental data on the Ge(105) surface, there is little direct evidence about the structure on hut-cluster facets, and almost nothing is known about how the facets of hut clusters, and hut clusters themselves, grow. In this paper, we show that there are at least two related structures for Ge(105) which we expect to be important during the growth of hut clusters. We also present details of the localized-orbital investigation we have used in preparation for linear-scaling density functional theory (DFT) calculations of full hut clusters.

The Ge/Si(001) system has been extensively studied as a prototypical example of hetero-epitaxial Stranski-Krastanov growth.³⁻⁵ There is also considerable technological interest in the system, because of its application in optoelectronic devices. The lattice parameter of bulk Ge is larger than that of Si by 4.2%. When Ge atoms are deposited on Si(001), growth initially occurs layer by layer, up to a critical thickness of about three monolayers. In this two-dimensional structure, strain due to the lattice mismatch is relieved by the formation of regularly spaced rows of dimer vacancies, resulting in the $2 \times N$ structure.⁶⁻⁸ It is reported that an $M \times N$ structure can follow this structure under some growth conditions.^{9,10} Deposition of further Ge leads to the forma-

tion of the three-dimensional (3D) pyramidlike structures called hut clusters.² The four facets of these hut clusters are well established to be $\{105\}$ surfaces. Deposition of still more Ge causes the formation of other 3D structures called “domes” having steeper facets.^{11,12} It is recognized that the stability of hut clusters must be governed by (a) the strain energy of the material in the clusters and in the underlying substrate and (b) the surface energy of the facets and to a lesser extent of the edges where the facets meet each other and the wetting layer. Since the $\{105\}$ facets in hut clusters are themselves strained by comparison with the (105) surface of unstrained Ge, the energetics of the strained Ge(105) surface is crucial to an understanding of the stability of hut clusters.

In spite of this importance of Ge(105), its equilibrium structure was speculative until recently. Initially, the paired-dimer (PD) model^{2,13} for this structure was proposed, as shown in Fig. 1(a). In this model, the paired dimers are separated by steps of the types called S_A and S_B . In S_A steps, dimer rows are parallel to the step, whereas in S_B , they are perpendicular. The S_B steps can, in general, be either unbonded or rebonded. In the paired-dimer model, they are unbonded. The dangling bonds present in this model are energetically unfavorable, and to overcome this the rebonded S_B step (RS), dimer model was proposed,¹⁴⁻¹⁶ where one dimer is added at the S_B step. This is illustrated in Fig. 1(b). Recently, the structure of Ge/Si(105) was studied by a combination of scanning tunneling microscopy (STM) measurements and DFT calculations by Fujikawa *et al.*¹⁵ They showed that RS model is more stable than the PD model, and this is supported by the agreement between STM images calculated using the RS model and experimental images.¹⁵⁻¹⁷ Interestingly and importantly, the DFT calculations showed

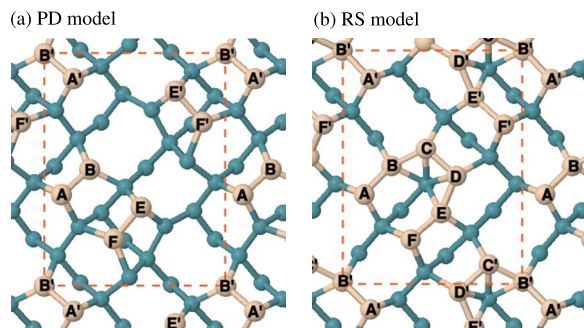


FIG. 1. (Color online) Structure of (a) PD model and (b) RS model of Ge(105) surface. Indices of the atoms of the dimers are also shown in the figures. Atoms C and D do not exist in a PD model.

that the RS model of Ge(105) is more stable than the Ge(001) surface when there is compression in the plane.^{18–20}

An approach that has been used in the past to model the similar huts that form when InAs is deposited on the GaAs (001) surface is to treat the material in the cluster and substrate by continuum elasticity theory and to treat only the energetics of the surface by DFT.^{21–23} For the stability of Ge/Si hut clusters, this hybrid approach was recently used by Shklyaeu *et al.*²⁴ and by Lu and Liu.²⁵ Both works reported that the energy difference between the strained Ge(105) facets and $2 \times N$ surfaces, although its sign is different between them, is very small. Because of this fact, they pointed out the important role of edge energies (that is, the energy due to sharp edges between facets), which are usually difficult to evaluate in such studies. Presumably, this hybrid approach, in which continuum and electronic-structure methods are combined, should become correct in the limit of very large nanostructures. However, to our knowledge, no information is available about the validity of this approach for the size of hut clusters studied experimentally. Certainly, for the smaller-scale structures believed to be involved in the nucleation of hut clusters, the validity of hybrid approaches must be in doubt. It therefore seems very desirable to attempt to model the entire hut-cluster system by a single modeling technique, preferably DFT. The ability to do this would make it possible to assess the errors of hybrid calculations. In fact, the energetics of Ge/Si huts has already been studied by Wagner and Gulari using a single atomistic method.²⁶ However, the accuracy of their empirical interatomic potentials for the energetics of the strained surfaces, the edges, and the top of the hut cluster is doubtful. These are the reasons why we wish to work toward a full DFT treatment of the entire hut clusters. In this paper, we present a careful investigation of the Ge(105) reconstruction with local orbital DFT methods and test the accuracy and validity of linear-scaling DFT for this system. This technique will be required for the DFT calculations on full hut clusters which are our final target and will be presented in a future work.

The development of DFT methods designed to work efficiently for very large systems has made rapid progress in the past few years. In particular, DFT techniques in which the computer effort and memory scale linearly with the number of atoms are now well established.^{27–31} This linear-scaling

capability, also called $O(N)$, is essential for modeling systems containing many thousands of atoms, because the steeper scaling of conventional electronic-structure techniques makes it difficult to apply them to systems of more than ~ 1000 atoms. An important feature of our own CONQUEST linear-scaling DFT code^{31–33} is that it can be operated at different levels of precision.³⁴ For rapid calculations, it employs atomiclike basis sets and can be run with or without electronic self-consistency. If greater accuracy is required, it can employ B spline basis sets,³⁵ which allow convergence to the basis-set limit in a way that closely resembles plane-wave techniques. Demonstrations of the practical linear-scaling capability of CONQUEST for systems of many thousands of atoms running on parallel computers were reported several years ago.^{36,37} Exploratory CONQUEST calculations on Ge/Si hut clusters have already been reported,³⁸ but these were designed only to test the feasibility of determining the electronic ground state of very large systems (we examined systems of up to 23 000 atoms). To have confidence in such calculations, it is clear that we must demonstrate their reliability both for strained bulk Si and Ge and for the energetics and equilibrium structure of the Ge(105) surface. This is one of the main aims of the present paper.

The rest of the paper is organized as follows. In the next section, we summarize the theoretical techniques, with the main emphasis on the $O(N)$ methods used on CONQUEST. In Sec. III, we then present our re-examination of the relaxed structures and energetics of the strained Ge(105) surface using a combination of tight-binding and plane-wave techniques. We shall point out there that the Ge(105) structures relevant to hut clusters may not be only those of lowest energy. We then (Sec. IV) report the work undertaken to test the validity of the localized-orbital and linear-scaling DFT methods. This work consists of several different parts: First, we examine unstrained and strained bulk Ge at the various levels of precision offered by CONQUEST, going from non-self-consistent DFT tight binding to full DFT at the basis-set limit. We then study strained Ge(105) using the same range of techniques. The final tests concern convergence with respect to the spatial cutoffs controlling $O(N)$ operation. The paper concludes (Sec. V) by discussing what the present work tells us about the prospects for accurate DFT calculations on large hut clusters using linear-scaling DFT techniques.

II. CALCULATION METHODS

The standard way of calculating relaxed surface structures and energies is by the plane-wave pseudopotential technique, and we use this in some of the present work. It is comprehensively outlined in books and reviews^{39,40} and needs no description here. We base our DFT-pseudopotential calculations on the local density approximation (LDA) using the standard Ceperley-Alder exchange-correlation functional. We choose to use LDA, rather than the generalized gradient approximation (GGA), because of evidence that surface formation energies are significantly more accurate with LDA than with GGA.⁴¹ We use Troullier-Martins norm-conserving pseudopotentials.⁴² The plane-wave pseudopotentials were

done using the STATE code.⁴³

The LDA calculations of Ge(105) surfaces used a slab geometry, though the number of layers in the slab was varied to ensure convergence of surface energy with slab depth. For all these calculations, the same simulation cell size was used, with a vacuum gap which was always at least 12.8 Å. The Brillouin zone was sampled using a $2 \times 3 \times 1$ mesh, and all calculations used a plane-wave cutoff energy of 16 Ry.

In addition to DFT, we have also made use of empirical tight-binding (TB) calculations, for two reasons. The first reason is that the cost of using CONQUEST for large complex systems is much reduced if an initial relaxed structure is first obtained with empirical TB. To do this in a controlled way, it is essential to know something about the accuracy of the TB model. The second reason is that TB gives a rapid way of exploring candidate structures, and we use it in this way for studying the Ge(105) surface. TB modeling has been reviewed extensively elsewhere.⁴⁴ The Si-Si parameters⁴⁵ and Ge-Ge and Ge-Si parameters⁴⁶ used here were fitted to the cohesive energies and bulk moduli, with the Si-Si parameters also fitted to the Si(001) surface. These parameters have been used previously for studies of both Si(001) and Ge/Si(001) and should be at least qualitatively reliable. The density matrix had a cutoff of three hops applied (where a hop is equivalent to a nearest-neighbor distance interaction).

Since localized-orbital and linear-scaling DFT methods are less well known, we give a brief summary here; for an overview of linear-scaling methods, Ref. 27 is useful, while Refs. 31 and 38 give details of the CONQUEST code. In the CONQUEST approach, the Kohn-Sham density matrix $\rho(\mathbf{r}, \mathbf{r}')$ is represented as

$$\rho(\mathbf{r}, \mathbf{r}') = \sum_{i\alpha, j\beta} \phi_{i\alpha}(\mathbf{r}) K_{i\alpha, j\beta} \phi_{j\beta}(\mathbf{r}'). \quad (1)$$

Here, the so-called support functions $\phi_{i\alpha}(\mathbf{r})$ (sometimes referred to as “localized orbitals” in related linear-scaling methods) are functions that are nonzero only inside “support regions” centered on the atoms, where i labels the atom and α runs over the support functions on a given atom; the coefficients $K_{i\alpha, j\beta}$ are the matrix elements of the density matrix in the (generally nonorthogonal) “basis” of support functions. In the CONQUEST code, the support regions are spheres of cutoff radius R_{reg} centered on the atoms. In general, the functions $\phi_{i\alpha}(\mathbf{r})$ can be varied and are themselves expressed in terms of basis functions. The present version of CONQUEST allows these basis functions to be either pseudoatomic orbitals or B splines (“blip” functions³⁵). For a given cutoff R_{reg} , the ground state is sought by minimizing the DFT total energy with respect to the density matrix $\rho(\mathbf{r}, \mathbf{r}')$, subject to the conditions that (a) ρ is weakly idempotent (its eigenvalues all lie between 0 and 1) and (b) ρ gives the correct number of electrons. With $\rho(\mathbf{r}, \mathbf{r}')$ expressed as in Eq. (1), this means that the $\phi_{i\alpha}(\mathbf{r})$ are optimized by variation of the coefficients of their expression in terms of basis functions, and the $K_{i\alpha, j\beta}$ are varied, subject to the two conditions just mentioned, until the minimum energy is found. Whatever freedom is allowed to the $\phi_{i\alpha}(\mathbf{r})$, their confinement to the support regions is a constraint, so that an upper bound to the ground-state energy,

rather than the ground-state energy itself, is obtained. This constraint can be progressively relaxed by letting $R_{\text{reg}} \rightarrow \infty$.

In practice, there are two distinct ways of obtaining the ground state. One way is, for fixed $\phi_{i\alpha}(\mathbf{r})$ and electron density, to replace variation of the $K_{i\alpha, j\beta}$ by the equivalent diagonalization of the Kohn-Sham Hamiltonian. Variation of the electron density to achieve self-consistency and variation of the $\phi_{i\alpha}(\mathbf{r})$ are performed in outer loops. This does not yield linear-scaling behavior, since diagonalization is an $O(N^3)$ operation. Nevertheless, this mode of operation will still be rapid for systems of up to a few hundred atoms. To achieve complete linear scaling, a cutoff must be imposed on the density matrix $K_{i\alpha, j\beta}$. The procedure used for this in CONQUEST is that of Li-Nunes-Vanderbilt (LNV),⁴⁷ in which K is expressed in terms of an “auxiliary density matrix” $L_{i\alpha, j\beta}$ by the matrix relation

$$K = 3LSL - 2LSLSL, \quad (2)$$

with $S_{i\alpha, j\beta} \equiv \langle \phi_{i\alpha} | \phi_{j\beta} \rangle$ the overlap matrix of support functions. A spatial cutoff R_L is then imposed on the L matrix: $L_{i\alpha, j\beta} = 0$ for $|\mathbf{R}_i - \mathbf{R}_j| > R_L$, where \mathbf{R}_i are the atomic positions. The reason why this procedure automatically yields weak idempotency is described in the original papers.

With either diagonalization or LNV linear scaling, the ground-state search is organized as three nested loops: (1) calculate the ground-state density matrix with fixed electron density and support functions, (2) vary the electron density to achieve self-consistency with fixed support functions, and (3) vary the support functions to achieve minimum energy.

This means that calculations can be done at different levels of precision. If only loop (1) is performed, we obtain non-self-consistent *ab initio* tight binding (hereafter, NSC-AITB), which is similar to empirical TB, except that now the matrix elements of the Hamiltonian and the other parts of the total energy are calculated from the given pseudopotentials and exchange-correlation energy, instead of being empirically parametrized. If only the first two loops are performed, we obtain self-consistent *ab initio* tight binding (SC-AITB). When all three loops are used, we obtain the self-consistent ground state in the basis used to represent the support functions. The blip basis set provides a flexibility equivalent to that of plane waves, so that if we allow $R_{\text{reg}} \rightarrow \infty$ and, in $O(N)$ operation, also $R_L \rightarrow \infty$, we recover the ground state that would be given by a plane-wave code. We will refer to calculations done with a large R_{reg} and an accurate blip basis set as “full DFT.”

In the following, plane-wave results for the energetics of Ge(105) provided by the STATE code are reported in the next section. CONQUEST calculations performed both by diagonalization and in $O(N)$ mode are reported in Sec. IV.

III. RELAXED STRUCTURES OF STRAINED Ge(105)

In this section, we investigate the stability of the strained Ge(105) surface, where the lattice parameters along the x and y ([100] and [010]) directions are set to the one of bulk silicon, a_{Si} . We noted in Sec. I that the rebonded-step (RS) structure of Ge(105) surface is believed to be more stable

TABLE I. Total energy of the six models of the strained Ge(105) surface calculated by semi-empirical TB and plane-wave LDA calculations. All energies are relative to the zigzag-A structure.

| Model | Buckling | | | | TB (meV/dimer) | LDA (meV/dimer) | Name |
|------------|----------|---|---|---|-------------------|--------------------|---------|
| | A | C | D | F | | | |
| Zigzag A | U | L | U | L | 0 | 0 | Type I |
| Zigzag B | L | U | L | U | 2 | 35 | |
| Parallel A | U | U | L | L | 68 | 80 | |
| Parallel B | L | L | U | U | 112 | 133 | |
| Flat A | U | L | L | U | 201 | -61 | Type II |
| Flat B | L | U | U | L | 211 | 245 | |

than the paired-dimer (PD) one. However, even within the RS model, there is another degree of freedom: how to arrange the buckling of the dimers. We recall that on the Si(001) and Ge(001) surfaces, the dimers making up the surface reconstruction are buckled in a Jahn-Teller distortion; a similar mechanism might be expected to apply here. As there are at least three independent dimers in the RS structure of Ge(105) [AB, CD, and EF atoms in Fig. 1(b) (Ref. 48)], it is likely that there would be several local minima with respect to the arrangement of the dimer bucklings. To our knowledge, however, only one structure has been reported in previous work. It is not clear whether this one is the ground state or only one of the local minima.⁴⁹ It is important to explore these structures for at least two reasons: first, the facets of Ge hut clusters on Si(001) will have a strain which may vary with position (high strain at the base of the hut and low strain near the top) and it may be that different strains affect the stabilities differently and, second, the different local minima may be important during growth of new layers of Ge(105) both on hut-cluster faces and on native Ge(105) surfaces.

In the Ge(105) RS model in Fig. 1(b), A, C, D, and F atoms are threefold coordinated atoms. Among these four atoms, we expect that two will become upper atoms (denoted as U) having sp^3 -like bonds, and the other two atoms will become lower atoms (denoted as L) having sp^2 type bonds. As a result, there are six cases to arrange the bucklings of the dimers in the RS model, which are classified into the following three types: (i) zigzag structure, atoms A and D are both U or both L, while atoms C and F both L or both U; (ii) parallel structure, atoms A and C are both U or both L and atoms D and F are both L or both U; and (iii) flat structure, atoms A and F are both U or both L and atoms C and D are both L or both U.

In this work, we have optimized the atomic positions and calculated the total energies for the six cases, first by using semiempirical TB calculations. Then, starting from the optimized atomic positions obtained by the semiempirical TB method, we have employed structure optimization using the plane-wave LDA method. As a result of the calculations, we have obtained six different locally or globally stable structures.

In order to model these (105) surfaces, we use a repeated slab model having the two equivalent surfaces in both ends. Surface unit cells are $[(-\frac{5}{2})a_{\text{Si}} \ 0 \ (\frac{1}{2})c_{\text{opt}}]$ and $[0 \ \alpha_{\text{Si}} \ 0]$. Here,

c_{opt} is the optimized lattice parameter along the z direction of the strained bulk Ge, whose lattice parameters along x and y are set to be a_{Si} (for more details, see Sec. IV B). In this section, we show the results for the slab with ten layers of Ge(105), which can be thought of as equivalent to eight Ge(001) monolayers with additional Ge atoms to make the vicinal surfaces. We have checked that the energy change by increasing the thickness of the slab is only a few meV per surface dimer.

The calculated energies by semiempirical TB and plane-wave LDA methods are shown in Table I; in each case, the energies are presented as an energy per surface dimer, relative to the most stable case. We can see that the relative stabilities of the zigzag and parallel structures by plane-wave calculations are qualitatively reproduced by the semiempirical TB calculations. The maximum forces calculated by plane-wave LDA calculations for the initial atomic positions, which were optimized by the TB calculations, are about $0.6 \text{ eV}/\text{\AA}$, which is small enough not to change the structure drastically. In the zigzag structures, the direction of the bucklings alternates along the dimer rows everywhere. For the zigzag-A structure, the tilt angle from the xy plane of the dimers CD, AB, and FE are 19.3° , 9.6° , and 9.6° , respectively. In the parallel structures, a dimer at the step edge (C and D atoms) also shows a buckling, but its direction is the same as that of the neighbor dimer and the degree of bucklings is smaller than that of zigzag structures. The tilt angle of the dimers CD, AB, and FE are 18.6° , 8.6° , and 8.0° , respectively, in parallel-A structure. This may explain why the parallel structures are less stable than the zigzag structures.

On the other hand, the heights of the two atoms of the dimer at the step edge are almost the same in the flat structures. From Table I, we can see that the present semiempirical TB calculations fail to reproduce the stability of the flat structures and the energy difference of the two flat structures, even qualitatively. Although its energy in the TB method is very high, the flat-A structure is the most stable in the plane-wave LDA calculations. This structure is the same as the one reported previously, and it has a feature that the changes of the heights at the step edges are small because the atoms (C and D) forming the dimer at the step edge are both lower atoms. As these two atoms are both upper atoms in the flat-B structure, the gap of the heights at the step edge is much larger in the flat-B structure. Therefore, the structures of

these two “flat” models are completely different and it is reasonable that LDA results show large energy difference between the stability of the two flat structures. (On the other hand, as we expect, the energy difference of the two zigzag structures and that of the two parallel structures are not large.) Although the TB calculations are not reliable for the energetics of the flat structures, the optimized structure by the method seems to be close to those by plane-wave LDA calculations. The *maximum* forces on an atom calculated using LDA for the optimized structures from the TB calculations are 1.26 and 0.52 eV/Å for the flat-A and flat-B structures, respectively. While these forces are sufficiently large to require further relaxation, they are not so large that they will result in a different local minimum structure after structural relaxation. This fact is important for our future large-scale DFT calculations on the Ge/Si(001) hut clusters, as it means that we will be able to obtain stable Ge {105} facets and avoid local minima problems by starting from TB relaxed structures.

Among the six structures, we consider two structures as important candidates for the facet structures of Ge/Si(001) hut clusters: the most stable, the flat-A structure, and the second most stable, the zigzag-A structure. Hereafter, we refer to the zigzag-A structure as type I and flat-A structure as type II structures, respectively.

There are two reasons why we consider the type I structure to be important. First, the energy difference between type I and the most stable structure (type II) is small. From the LDA calculations of the various structures of the Ge(001) surface reported in Ref. 50, we can see that the energy gain to make the buckled (asymmetric) dimer and the one by forming a zigzag structure are 294 and 87 meV/dimer, respectively. These values are much larger than the energy difference between the type I and II structures. Considering that the flip-flop motion of the dimers in the Ge(001) surface occurs at room temperature, it may be possible that the stability of types I and II would change if we introduce entropic effects. Furthermore, these structures may well be important for growth of Ge(105) facets: When one or a few Ge adatoms are put on the surfaces, the order of the stability of the surfaces may change.

Second, the type I structure may well be important for the structure of hut-cluster faces near the edges. The buckling of the type I (zigzag-A) structure can be determined locally for each dimer pair, while three dimers are required to obtain the buckling of the type II structure; in this sense, the type II structure is nonlocal and cannot accommodate irregular sites, such as impurities or edges of the faces. As the area of the facets of Ge/Si(001) hut clusters is finite and not large enough to treat them as infinite surfaces, we cannot neglect the effect of the end of the facets. Thus, we think that type I surface may be more stable as the facets of the Ge/Si(001) hut clusters, especially for the small ones. The structural model of zigzag B is also stable in energy. However, the structural feature of this model is almost the same as that of zigzag A and it is enough to study the type I structure only.

The optimized structures of the type I and II surfaces are shown in Fig. 2, and their structural parameters are listed in Table II. To ensure that these results are not an artifact of the functional chosen, we have also calculated the stabilities us-

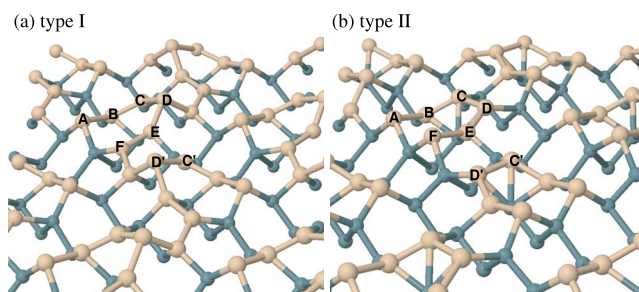


FIG. 2. (Color online) Two types of Ge(105) surface structures. Indices of atoms are same as those in Fig. 1(b).

ing GGA. The energy *difference* between the two structures is almost the same (51 meV/dimer); however, the absolute values of the surface energies are rather different.

IV. LOCALIZED-ORBITAL DENSITY FUNCTIONAL THEORY

In this section, we investigate the accuracies of the different methods offered by CONQUEST, namely, NSC-AITB, SC-AITB, and full DFT calculations, for unstrained and strained Ge (these different levels of calculation are outlined in Sec. II). The reliable calculation conditions for the full DFT calculations by CONQUEST are also examined here. As the accuracies of the different methods and the calculation condition for the full DFT calculations by CONQUEST are not related to the $O(N)$ method, we study them by using a diagonalization technique. The accuracy and the calculation conditions introduced by the $O(N)$ method are investigated only in Sec. IV D.

Here, we need to make a comment for the basis set used for the NSC-AITB and SC-AITB calculations. For these calculations, we first need to define a set of localized orbitals to express the support functions, and we use a single zeta basis set of pseudoatomic orbitals (PAOs) in this study because its calculation cost is low. In the choice of the single zeta basis set, we have a degree of freedom for the localization of the PAOs (or energy shift in the context of SIESTA code²⁸). For our study on Ge/Si systems, it is important to reproduce the lattice mismatch between the Ge and Si systems. In addition to this, there is a problem in LDA or GGA calculations for the semiconducting bulk Ge that the band structure shows a metallic behavior if we use a lattice parameter slightly larger than the experimental one; as well as being unphysical, this will be particularly bad for $O(N)$ calculations which rely on the locality of the density matrix. From these reasons, we have decided to use PAOs, which reproduce the *experimental* lattice parameter of bulk Ge and bulk Si by the SC-AITB method. The accuracy of our NSC-AITB and SC-AITB methods depends on the present choice of the localized-orbital basis sets, and we show them for the unstrained or strained Ge systems in the following sections.

A. Bulk germanium

We start from the simplest system, that is, unstrained bulk Ge with diamond structure. Figure 3 shows the total energy

TABLE II. Structural parameters of the two strained Ge(105) surfaces, whose structures are optimized by plane-wave LDA calculations. For the indices of atoms, see Fig. 1(b).

| Type | Sum of bond angles (deg) | | | | Bond length (Å) | | | | |
|------|--------------------------|-------|-------|-------|-----------------|------|------|------|------|
| | A | C | D | F | AB | BC | CD | DE | EF |
| I | 283.6 | 355.7 | 280.5 | 349.9 | 2.58 | 2.40 | 2.50 | 2.56 | 2.51 |
| II | 286.0 | 339.5 | 346.8 | 285.0 | 2.54 | 2.41 | 2.44 | 2.43 | 2.56 |

of bulk Ge as a function of the lattice parameter using NSC-AITB and SC-AITB methods. The experimental lattice parameter is 5.654 Å, and, as we have already mentioned, the present basis set is chosen so that the optimized one by the SC-AITB is close to the experimental value (+0.2%). From Fig. 3, we can see that the optimized lattice parameter from the NSC-AITB method is about 0.4% larger than the experimental value, which is very good agreement.

Next, we perform full DFT calculations of bulk Ge using CONQUEST. When the support functions are represented by a basis of B splines (blip functions), there are two independent parameters which control the accuracy of the method: the region radius of the support functions R_{reg} and the spacing of the cubic grid on which the blips are defined, known as the blip-grid spacing b .

We first study the region radius dependence of the total energy. Figure 4 shows the total energy of bulk Ge with the experimental lattice parameter as a function of R_{reg} using the fixed blip-grid spacing $b=0.34$ Å. From the figure, we can see that the error of the total energy of bulk Ge is smaller than 0.2 eV/atom if we use R_{reg} larger than 3.8 Å. This is about 7 mhartree/atom, which is comparable to the tolerances used, for instance, when creating ultrasoft pseudopotentials, and should be acceptable. However, it should be noted that it is unclear how these errors will change when we calculate different Ge systems.

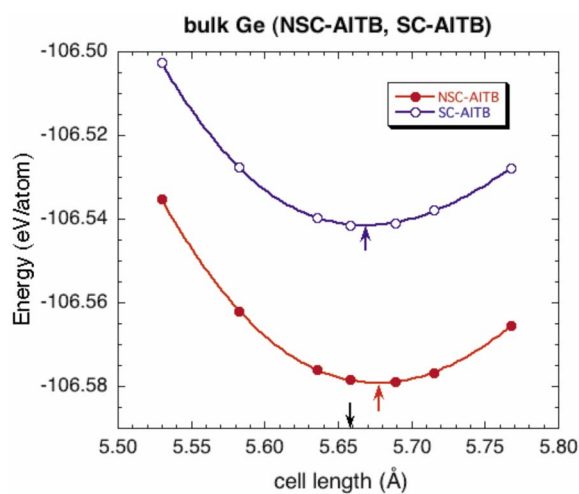


FIG. 3. (Color online) Total energy of bulk Ge as a function of a cell length calculated by NSC-AITB (closed circles) and SC-AITB (open circles) methods. The arrows pointing to the curves show the minimum points, while the arrow pointing to the horizontal axis corresponds to the experimental cell length.

Next, we examine the total energy dependence on the blip-grid spacing. Figure 5 shows the total energy of bulk Ge obtained by using different blip-grid spacings b , with the fixed region radius $R_{\text{reg}}=3.85$ Å. Here, the horizontal axis is expressed by a cutoff energy which is defined³⁵ as $E_{\text{cut}} = \hbar^2(\frac{\pi}{b})^2/2m_e$. The total energy as a function of the lattice parameter, with several blip-grid spacings, is illustrated in Fig. 6. From these figures, as we have expected, we can see the convergence property with respect to blip-grid spacing is similar to the one in the usual plane wave calculations with respect to cutoff energies. If we use coarse blip grids, which corresponds to using small cutoff energies in plane-wave calculations, the optimized cell length is larger than the converged value. We can see that the converged optimized cell length (-1.0% of the experimental cell length) is close to other LDA calculations.^{51,52} From Figs. 5 and 6, we can conclude that $b=0.34$ Å is reliable enough for the blip-grid spacing. The errors in the total energy using this value as a blip-grid spacing is less than 0.13 eV/atom (or about 4 mhartree/atom). We expect that the errors in relative energies will be much smaller than this, because the above error in total energy mainly comes from the core region, and will be the same in different environments. We note that typical plane-wave calculations rarely, if ever, use fully converged energies, instead of relying on converged energy differences.

B. Strained bulk germanium by non-self-consistent *ab initio* tight-binding, self-consistent *ab initio* tight-binding, and full density functional theory methods

We are ultimately interested in the Ge/Si(001) system. For the Ge layers or hut clusters on Si(001), the Ge-Ge in-

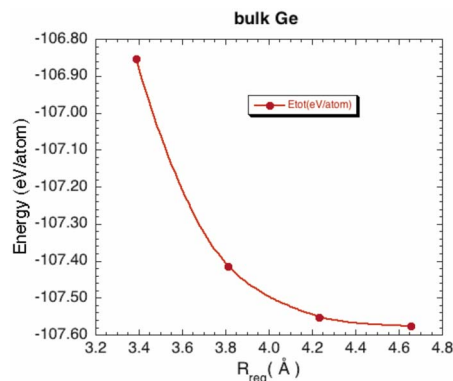


FIG. 4. (Color online) Dependence of the total energy of bulk Ge on region radius R_{reg} , calculated by full DFT method using blip functions.

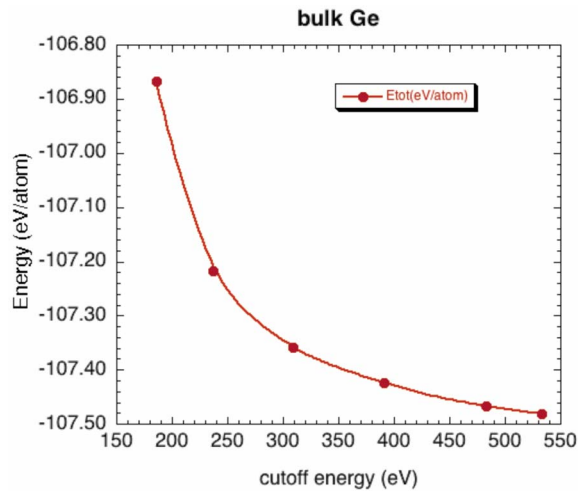


FIG. 5. (Color online) Dependence of the total energy of bulk Ge on blip-grid spacing, calculated by full DFT method using blip functions. Blip-grid spacing is transformed to a corresponding cutoff energy.

tralayer spacing is compressed along the x and y directions by the silicon lattice parameter. As a result, the interlayer distance along the z direction should be elongated to minimize the energy with this constraint. In this section, we show how accurate the different methods are to reproduce this situation quantitatively.

We have calculated the total energy of the strained bulk germanium, whose lattice parameters along the x and y directions are fixed as the experimental lattice parameter of bulk silicon, a_{Si} . Three different methods, NSC-AITB, SC-AITB, and full DFT, are employed and the total energy is calculated as a function of c (the lattice parameter along the z direction). The resulting energy curves are shown in Fig. 7. We can see that the optimized length of c (c_{opt}) is almost the same for both NSC-AITB and SC-AITB methods: c_{opt} is

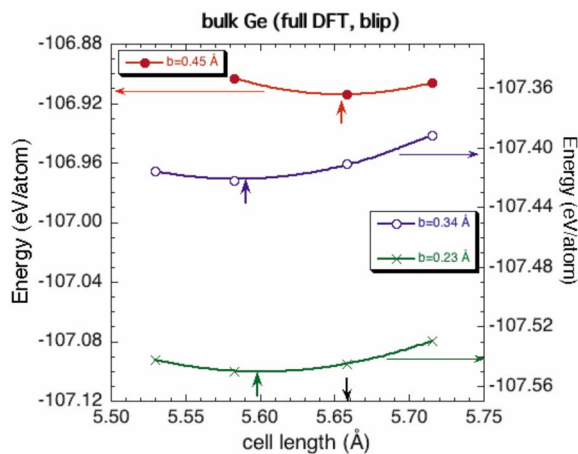


FIG. 6. (Color online) Total energy of bulk Ge as a function of a cell length obtained by full DFT calculations using blip functions, with different blip-grid spacings. The arrows pointing to the curves show the minimum points, while the arrow pointing to the horizontal axis corresponds to the experimental cell length.

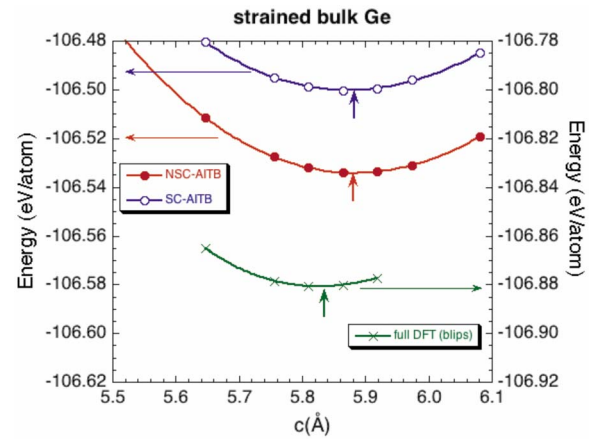


FIG. 7. (Color online) Total energy of strained bulk Ge as a function of a interlayer cell length (along the z direction). Cell lengths along the x and y directions are compressed to the lattice parameter of silicon. The curves with filled and open circles show the results by NSC-AITB and SC-AITB methods, respectively, while the one with crosses shows the result by full DFT method using blip functions. The arrows pointing to the curves show the minimum points for each method.

$1.082a_{\text{Si}}$ for NSC-AITB, while it is $1.081a_{\text{Si}}$ for SC-AITB. The curvature of the energy around c_{opt} is also similar in both methods. On the other hand, for full DFT calculations using a blip function basis with $R_{\text{reg}}=3.85 \text{ \AA}$ and $b=0.34 \text{ \AA}$, we find that c_{opt} is $1.075a_{\text{Si}}$. We think that this small difference is mainly due to the optimized cell length of bulk germanium by a full DFT calculation being slightly smaller than the one obtained by NSC-AITB or SC-AITB calculations, so that the degree of the compression is smaller in full DFT calculations. As we are concerned with comparing different methods, it is sensible to reduce the number of differences between calculations, and we therefore use the same value for the strain in all cases. Apart from this small difference, we can conclude that SC-AITB or even NSC-AITB calculations are able to reproduce the energetics of this strained bulk germanium system to an accuracy of 1%.

C. Optimized structure and surface energy of strained Ge(105) by non-self-consistent *ab initio* tight-binding, self-consistent *ab initio* tight-binding, and full density functional theory methods

Next, we study the stability of the strained surface Ge(105) shown in Sec. III. The purpose of this section is to clarify the accuracy of the different methods to calculate the optimized structure, surface energy, and the relative stabilities of the strained Ge(105) surfaces. As in Sec. III, one of the lengths of the surface unit cell of Ge(105) is $\sqrt{(\frac{5}{2}a_{\text{Si}})^2 + (\frac{1}{2}c_{\text{opt}})^2}$. Strictly speaking, the unit cell of Ge(105), which are intended to reproduce the Ge {105} facets grown on the Si(001) surface, should be calculated with the optimized c length c_{opt} calculated in the last section. However, for all calculations in this work, we use the value found using SC-AITB, $c_{\text{opt}}=1.081a_{\text{Si}}$, because the difference of c_{opt}

TABLE III. Structural parameters of the type I strained Ge(105) surface optimized by different methods. For the indices of atoms, see Fig. 1(b).

| Type | Sum of bond angles (deg) | | | | Bond length (Å) | | | | |
|-------------------------------------|--------------------------|-------|-------|-------|-----------------|------|------|------|------|
| | A | C | D | F | AB | BC | CD | DE | EF |
| Semiempirical | 283.3 | 350.3 | 273.3 | 346.3 | 2.64 | 2.49 | 2.53 | 2.59 | 2.54 |
| NSC-AITB | 284.6 | 354.0 | 277.9 | 349.4 | 2.57 | 2.43 | 2.53 | 2.56 | 2.54 |
| SC-AITB | 276.9 | 355.2 | 273.7 | 351.0 | 2.59 | 2.44 | 2.56 | 2.59 | 2.55 |
| Full DFT ($R_{\text{reg}}=3.85$ Å) | 281.8 | 355.7 | 278.2 | 349.5 | 2.59 | 2.39 | 2.51 | 2.57 | 2.53 |
| Plane wave | 283.6 | 355.7 | 280.5 | 349.9 | 2.58 | 2.40 | 2.50 | 2.56 | 2.51 |

by different methods is very small and this will make comparisons considerably easier. It is important to note that, even if we considered Ge(105) on Si(105) and thus used $c_{\text{opt}}=a_{\text{Si}}$, the length is $5.099a_{\text{Si}}$ and its difference from the value in this work, $5.1155a_{\text{Si}}$, is very small.

The structural parameters of the optimized atomic positions of the type I Ge(105) surface calculated using different methods are shown in Table III. For comparison, the result calculated by a semiempirical TB method and the one by the plane-wave code STATE⁴³ are also shown in the table. From the table, we can see first that the agreement between the result by full DFT with blip functions by CONQUEST and the one by the plane-wave method is almost perfect. The optimized structures by SC- and NSC-AITB methods also agree well with the result from the plane-wave method, but the differences from the plane-wave result, especially those in the bond lengths, are larger. We also find that the optimized structures calculated using SC- and NSC-AITB are almost the same. The semiempirical method can also give good results, but the differences from the plane-wave result are larger than those by NSC- or SC-AITB methods. These results suggest that if we start from the semiempirical method and switch to NSC- or SC-AITB method and then to full DFT method, we can increase the accuracy of the optimized atomic positions step by step. A detailed comparison of the CPU time required for the different methods, while interesting, is rather difficult to perform: for linear-scaling techniques, the time required depends on the accuracy chosen. We are working on this problem and will present details in a future publication; however, as a guide going from empirical tight binding to NSC-AITB requires about ten times as much CPU time, while going from NSC-AITB to full DFT again requires about ten times the CPU time.

Next, we move to the surface energy. One standard method for calculating surface energy is to evaluate the total energy of slabs of different thicknesses until the change in energy between successive calculations is a constant; a linear fit can be made to these energies whose intercept gives the surface energy. For the NSC-AITB case, we have performed such a fit and have found that the convergence is such that only two calculations are required to give the surface energy; these have slabs of eight or ten (001) monolayers with extra Ge atoms added to make the vicinal surfaces. The calculated surface energies of the type I structure obtained by different methods are shown in Table IV, together with the results by semiempirical TB and plane-wave LDA methods.

For the full DFT calculations with blip functions by CONQUEST, we have found that the surface energy is sensitive to the region radius R_{reg} , although the optimized atomic positions are almost the same. The reduction of the surface energy by changing R_{reg} from 3.85 to 4.23 Å is large and is about 8.7 meV/Å². We expect that a further increase of the region radius would result in the reduction of the surface energy. On the other hand, increasing the cutoff energy in the plane-wave calculations would increase the surface energy,¹⁸ though it should be less than a few meV/Å². Considering these aspects and that CONQUEST and STATE use different pseudopotentials, we can say that the result by full DFT with blip functions is very close to the one by the plane-wave code.

Moving from the blip basis to the minimal PAO basis, we see in Table IV that NSC-AITB appears to agree with full DFT rather better than SC-AITB. However, this must be due to a happy cancellation of errors (which DFT, in general, makes use of), as full charge self-consistency must give a more accurate description of a given system in general. This cancellation appears to be transferable: When considering the energy difference between the type I and type II structures, which is 61 meV/dimer from full DFT, NSC-AITB gives 39 meV/dimer (with the same signs) while SC-AITB gives 6 meV/dimer (with the opposite signs). This poor performance of SC-AITB must be related to the minimal basis: with a more complete basis set, the agreement would improve. We conclude that, due to a fortuitous cancellation of errors, NSC-AITB with the present basis set is reliable for strained Ge(105) surfaces and will give surface energies correct to a few percent, while SC-AITB is not reliable. Our

TABLE IV. Surface energy of the type I strained Ge(105) surface. The result by a semiempirical TB method and the one by plane-wave calculations are also listed for comparison.

| Method | Surface energy (meV/Å ²) |
|---|--------------------------------------|
| Semiempirical | 74.3 |
| NSC-AITB | 76.5 |
| SC-AITB | 81.5 |
| Full DFT (blips, $R_{\text{reg}}=3.85$ Å) | 83.5 |
| Full DFT (blips, $R_{\text{reg}}=4.23$ Å) | 74.8 |
| Plane wave | 71.0 |

calculations of the stabilities of Ge hut clusters on Si(001) will proceed on this basis.

In the end of this section, we report the strain dependence of the surface energy of Ge(105) obtained by different methods. It has been previously reported that the surface energy of Ge(105) type II surface is greatly reduced by compression.^{18,19} On the other hand, the reduction of the surface energy by strain cannot be reproduced by the empirical interatomic potential calculations.¹⁹ Thus, it is important to clarify how reliable the NSC-AITB method is to reproduce the stability of the surface energy at different compressions. It is also interesting to investigate the change of the surface energy of type I structure, as this surface has not been reported. For these purposes, we calculate the surface energy of type I and II structures using two values as a lattice parameter along the x and y directions; one is the experimental lattice parameter of bulk silicon as in the previous (and present) section, and the other one is the experimental one of bulk germanium, corresponding to the uncompressed case.

First, we calculate the surface energies by using plane-wave LDA method. For the type II structure, the reduction of the surface energy by the compression is $3.9 \text{ meV}/\text{\AA}^2$, changing from 73.2 to $69.3 \text{ meV}/\text{\AA}^2$. In Ref. 19, the corresponding value is about $6 \text{ meV}/\text{\AA}^2$. However, these values are often sensitive to the lattice parameter chosen and the parameters used in calculations, and this level of agreement is rather good. For the type I structure, we have found that the change of the surface energy is almost the same, $4.0 \text{ meV}/\text{\AA}^2$, changing from 7.50 to $71.0 \text{ meV}/\text{\AA}^2$. The present result shows that the relative stability of the two surfaces is almost unchanged by the compression.

If we use the NSC-AITB method to calculate the surface energy, the calculated surface energy changes from 83.5 to $75.6 \text{ meV}/\text{\AA}^2$ for the type II surface, and the reduction of the surface energy is $7.9 \text{ meV}/\text{\AA}^2$. For the type I surface, it changes from 8.50 to $76.5 \text{ meV}/\text{\AA}^2$, and the reduction is $8.5 \text{ meV}/\text{\AA}^2$. Although we have small quantitative errors in the NSC-AITB method, it successfully reproduces two important aspects: (1) large reduction of the surface energy by compression and (2) the strain dependence of the surface energy being almost the same for type I and II surfaces.

Finally, we comment on the results from the semiempirical TB method. As we have reported in Sec. III, this method cannot reproduce the relative stability of type II structure. However, we have found that the reduction in surface energy following compression mentioned above is reproduced by the method. For type I surface, the surface energy changes from 79.4 to $75.5 \text{ meV}/\text{\AA}^2$ and the change is $3.9 \text{ meV}/\text{\AA}^2$. On the other hand, for type II structure, the change is much smaller than the one by plane-wave LDA method. The reduction of the surface energy by the compression is only $2.0 \text{ meV}/\text{\AA}^2$. Although we have such errors in the semiempirical TB method, we think that the method is much more accurate than the method by empirical interatomic potentials for the stability of the strained Ge(105) surface.

D. Accuracy and calculation condition in linear-scaling density functional theory calculations on strained Ge(105)

In this section, we introduce another type of approximation, which is needed to realize the $O(N)$ method. As ex-

plained in Sec. II, the only parameter which controls the accuracy of the $O(N)$ method by CONQUEST is the cutoff radius of the auxiliary density matrix, R_L . Our main concern here is to get the information about the accuracy and reliable calculation condition for our future study on the Ge/Si(001) hut-cluster systems.

The localization of the density matrix is closely related to the energy gap of the system. We need smaller cutoff ranges of the auxiliary density matrix R_L for the systems having larger energy gap. On the bulk silicon or carbon systems or on those including a single impurity site, we showed the R_L dependence of the total energy.^{32,31} In a Ge/Si(001) hut-cluster system with a wetting layer, as all the Si atoms are four coordinated, we expect that the local density of states for the Si substrate has a certain energy gap. On the other hand, there are many threefold coordinated Ge atoms in the facets of the hut cluster and the local density of states near the facets is expected to have a narrower energy gap. Thus, we expect that the reliable cutoff R_L is mainly determined near the facets of the Ge hut cluster. In this section, we study the accuracy and the reliable calculation condition of the strained Ge(105) surfaces. These results will help us to evaluate appropriate simulation parameters for our future $O(N)$ study on the Ge/Si(001) hut clusters. As we expect, the R_L dependences of the total energy, forces, or the surface energy are almost the same between NSC-AITB, SC-AITB, and full DFT methods, and we use NSC-AITB method in this work.

We have performed $O(N)$ NSC-AITB calculations on the type I and II structures of the Ge(105) surfaces shown in Sec. III. For both systems, we use the atomic positions which are optimized by a diagonalization method with the force criterion of $0.1 \text{ mhartree/bohr}$ ($=0.0058 \text{ eV}/\text{\AA}$). We have optimized the density matrix using different R_L and have calculated the total energy and forces. The surface energy is also calculated by using the total energy of the two Ge(105) systems having eight or ten layers. Table V shows the total energy and the maximum force for the ten-layer system and the surface energy. For comparison, the results obtained by diagonalization are also presented.

As we use the optimized atomic positions by the diagonalization method, the maximum force should become smaller if we use larger R_L . In addition, if we increase R_L , the total energy should be lower and closer to the value obtained by diagonalization. The results in Table V clearly show these behaviors. From the table, we can see that the error in the total energy for the both surfaces is 0.03 eV/atom if we use $R_L=10.8 \text{ \AA}$. We can expect error cancellations for the difference of the energy, and, in fact, the calculated surface energy is already almost converged if we use $R_L=10.8 \text{ \AA}$. The energy difference between the type I and II surfaces is also well converged at $R_L=10.8 \text{ \AA}$, which is 37 meV/dimer , while it is 39 meV/dimer by the diagonalization. The errors in forces are also small if we use R_L larger than 10.8 \AA . From these results, we can conclude that $R_L=10.8 \text{ \AA}$ is a reliable cutoff for the strained Ge(105) surfaces.

V. CONCLUSION

In this paper, we have performed a DFT study on the strained Ge(105) surface. The surface is observed as a facet

TABLE V. Total energy E_{tot} , maximum of the force component on atoms f_{max} , and surface energy E_{surf} for the type I and II strained Ge(105) surfaces calculated using the $O(N)$ method (NSC-AITB level) with different cutoff distances R_L . The results obtained by an exact diagonalization (labeled diag) is also shown.

| R_L (Å) | Type I | | | Type II | | |
|--------------|-------------------------------|----------------------------|--|-------------------------------|----------------------------|--|
| | E_{tot} (eV/atom) | f_{max} (eV/Å) | E_{surf} (meV/Å ²) | E_{tot} (eV/atom) | f_{max} (eV/Å) | E_{surf} (meV/Å ²) |
| 8.2 | -106.381 | 0.1398 | 80.1 | -106.384 | 0.1372 | 78.1 |
| 10.8 | -106.442 | 0.0766 | 75.3 | -106.446 | 0.0597 | 74.1 |
| 13.4 | -106.464 | 0.0404 | 75.2 | -106.468 | 0.0343 | 73.9 |
| 16.1 | -106.472 | 0.0223 | 75.5 | -106.476 | 0.0228 | 74.3 |
| diag | -106.477 | 0.0058 | 76.5 | -106.481 | 0.0058 | 75.5 |

of Ge 3D islands on Si (001), and the present study is motivated by the desire to study these nanostructured systems using DFT methods. This work can be divided into two parts: (i) modeling of the strained Ge(105) surface and (ii) investigation of the use of localized orbitals for the strained Ge systems.

In the first part of the present study, using a combination of tight-binding and pseudopotential and/or plane-wave DFT calculations, we have considered the effect of buckling of surface dimers on the stability and form of the reconstructed Ge(105) surface. We have presented the total energy of six possible relaxed structures of the strained Ge(105) surface and have shown that the two lowest energy structures are important for modeling of Ge {105} facets in the Ge/Si hut clusters. The energy difference between these two structures is only 61 meV/dimer. It was also pointed out that it will be much easier to form irregular sites, such as the edges of the surfaces, with the second most stable structure rather than the most stable structure, owing to the locality of its buckling.

In the second part, for unstrained or strained Ge systems, we have examined and clarified the accuracy of several DFT methods, such as NSC-AITB, SC-AITB, and full DFT methods, which we can employ with localized-orbital basis sets. It has been demonstrated that the DFT calculations with localized orbitals using B-spline basis sets (blip functions) can reproduce the results by pseudopotential and/or plane-wave DFT methods very accurately. We have also shown that, owing to a fortuitous cancellation of errors, the NSC-AITB

method is reliable for calculating the stabilities of different strained Ge systems, including Ge(105) surface. These facts are very encouraging for our ongoing study on the Ge/Si(105) systems. Note that it is straightforward to switch from the NSC-AITB method to a more accurate method using our linear-scaling DFT code CONQUEST. The applicability of linear-scaling DFT methods for this system has also been studied in this paper. We have found that linear-scaling DFT results are well converged for a cutoff radius on the auxiliary density matrix larger than 10.8 Å.

We already showed in our previous work that it is now possible to do DFT calculations on the systems containing more than 10 000 atoms.^{36,38} This ability, coupled with the results shown in the present paper, makes us confident that we are now ready to perform DFT calculations on a nanostructured Ge/Si system, which includes the entire Ge hut cluster as well as the silicon substrate. Results of this study will be presented in a future publication.

ACKNOWLEDGMENTS

We acknowledge T. Ohno for fruitful discussion and his support on CONQUEST project. The calculations in this work were performed by using the numerical materials simulator at NIMS and the facilities of the Cybermedia Center at Osaka University and the Earth Simulator Center. D.R.B. is supported by the Royal Society, and R.C. by EPSRC. This work is partly supported by Grant-in-Aid for Scientific Research from the MEXT, Japan.

*miyazaki.tsuyoshi@nims.go.jp

†david.bowler@ucl.ac.uk

‡Present address: Department of Physics, Kings College London, Strand, London WC2R 2LS, United Kingdom.

§m.gillan@ucl.ac.uk

¹C. Teichert, Phys. Rep. **365**, 335 (2002).

²Y. W. Mo, D. E. Savage, B. S. Swartzentruber, and M. G. Lagally, Phys. Rev. Lett. **65**, 1020 (1990).

³F. Liu, F. Wu, and M. G. Lagally, Chem. Rev. (Washington, D.C.) **97**, 1045 (1997).

⁴V. A. Shchukin and D. Bimberg, Rev. Mod. Phys. **71**, 1125

(1999).

⁵J.-M. Baribeau, X. Wu, N. L. Rowell, and D. J. Lockwood, J. Phys.: Condens. Matter **18**, R139 (2006).

⁶Y. W. Mo and M. G. Lagally, J. Cryst. Growth **111**, 876 (1991).

⁷U. Köhler, O. Jusko, B. Müller, M. von Hoegen, and M. Pook, Ultramicroscopy **42-44**, 832 (1992).

⁸J. Oviedo, D. R. Bowler, and M. J. Gillan, Surf. Sci. **515**, 483 (2002).

⁹I. Goldfarb, P. T. Hayden, J. H. G. Owen, and G. A. D. Briggs, Phys. Rev. Lett. **78**, 3959 (1997).

¹⁰K. Li, D. R. Bowler, and M. J. Gillan, Surf. Sci. **526**, 356 (2003).

- ¹¹G. Medeiros-Ribeiro, A. M. Bratkovski, T. I. Kamins, D. A. A. Ohlberg, and R. S. Williams, *Science* **279**, 353 (1998).
- ¹²F. M. Ross, R. M. Tromp, and M. C. Reuter, *Science* **286**, 1931 (1999).
- ¹³M. Tomitori, K. Watanabe, M. Kobayashi, and F. Iwasaki, *Surf. Sci.* **301**, 214 (1994).
- ¹⁴K. E. Khor and S. D. Sarma, *J. Vac. Sci. Technol. B* **15**, 1051 (1997).
- ¹⁵Y. Fujikawa, K. Akiyama, T. Nagao, T. Sakurai, M. G. Lagally, T. Hashimoto, Y. Morikawa, and K. Terakura, *Phys. Rev. Lett.* **88**, 176101 (2002).
- ¹⁶P. Raiteri, D. B. Migas, L. Miglio, A. Rastelli, and H. von Känel, *Phys. Rev. Lett.* **88**, 256103 (2002).
- ¹⁷T. Hashimoto, Y. Morikawa, Y. Fujikawa, T. Sakurai, M. G. Lagally, and K. Terakura, *Surf. Sci.* **513**, L445 (2002).
- ¹⁸T. Hashimoto, Y. Morikawa, and K. Terakura, *Surf. Sci.* **576**, 61 (2005).
- ¹⁹D. B. Migas, S. Cereda, F. Montalenti, and L. Miglio, *Surf. Sci.* **556**, 121 (2004).
- ²⁰G.-H. Lu, M. Cuma, and F. Liu, *Phys. Rev. B* **72**, 125415 (2005).
- ²¹E. Pehlke, N. Moll, A. Kley, and M. Scheffler, *Appl. Phys. A: Mater. Sci. Process.* **65**, 525 (1997).
- ²²L. G. Wang, P. Kratzer, M. Scheffler, and N. Moll, *Phys. Rev. Lett.* **82**, 4042 (1999).
- ²³L. G. Wang, P. Kratzer, N. Moll, and M. Scheffler, *Phys. Rev. B* **62**, 1897 (2000).
- ²⁴O. E. Shklyaev, M. J. Beck, M. Asta, M. J. Miksis, and P. W. Voorhees, *Phys. Rev. Lett.* **94**, 176102 (2005).
- ²⁵G.-H. Lu and F. Liu, *Phys. Rev. Lett.* **94**, 176103 (2005).
- ²⁶R. J. Wagner and E. Gulari, *Surf. Sci.* **590**, 1 (2005).
- ²⁷S. Goedecker, *Rev. Mod. Phys.* **71**, 1085 (1999).
- ²⁸J. M. Soler, E. Artacho, J. D. Gale, A. García, J. Junquera, P. Ordejón, and D. Sánchez-Portal, *J. Phys.: Condens. Matter* **14**, 2745 (2002).
- ²⁹C.-K. Skylaris, P. D. Haynes, A. A. Mostofi, and M. C. Payne, *J. Chem. Phys.* **122**, 084119 (2005).
- ³⁰T. Ozaki, *Phys. Rev. B* **74**, 245101 (2006).
- ³¹D. R. Bowler, T. Miyazaki, and M. J. Gillan, *J. Phys.: Condens. Matter* **14**, 2781 (2002).
- ³²E. Hernández and M. J. Gillan, *Phys. Rev. B* **51**, 10157 (1995).
- ³³E. Hernández, M. J. Gillan, and C. M. Goringe, *Phys. Rev. B* **53**, 7147 (1996).
- ³⁴T. Miyazaki, D. R. Bowler, R. Choudhury, and M. J. Gillan, *J. Chem. Phys.* **121**, 6186 (2004).
- ³⁵E. Hernández, M. J. Gillan, and C. M. Goringe, *Phys. Rev. B* **55**, 13485 (1997).
- ³⁶D. R. Bowler, T. Miyazaki, and M. J. Gillan, *Comput. Phys. Commun.* **137**, 255 (2001).
- ³⁷C. M. Goringe, E. Hernández, M. J. Gillan, and I. J. Bush, *Comput. Phys. Commun.* **102**, 1 (1997).
- ³⁸D. R. Bowler, R. Choudhury, M. J. Gillan, and T. Miyazaki, *Phys. Status Solidi B* **243**, 989 (2006).
- ³⁹R. M. Martin, *Electronic Structure: Basic Theory and Practical Methods* (Cambridge University Press, Cambridge, UK, 2004).
- ⁴⁰M. C. Payne, M. P. Teter, D. C. Allan, T. A. Arias, and J. D. Joannopoulos, *Rev. Mod. Phys.* **64**, 1045 (1992).
- ⁴¹Because of the paucity of reliable experimental values for surface formation energies, it is difficult to be certain whether LDA or GGA gives better predictions. Evidence that LDA tends to be better than GGA for surface formation energies is presented in Refs. 53–55.
- ⁴²N. Troullier and J. L. Martins, *Phys. Rev. B* **43**, 1993 (1991).
- ⁴³Y. Morikawa, *Phys. Rev. B* **63**, 033405 (2001).
- ⁴⁴C. M. Goringe, D. R. Bowler, and E. H. Hernández, *Rep. Prog. Phys.* **60**, 1447 (1997).
- ⁴⁵D. R. Bowler, M. Fearn, C. M. Goringe, A. P. Horsfield, and D. G. Pettifor, *J. Phys.: Condens. Matter* **10**, 3719 (1998).
- ⁴⁶D. R. Bowler, *J. Phys.: Condens. Matter* **14**, 4527 (2002).
- ⁴⁷X.-P. Li, R. W. Nunes, and D. Vanderbilt, *Phys. Rev. B* **47**, 10891 (1993).
- ⁴⁸The dimers in different parts of the surface, as indicated by AB and A'B', for example, do *not* have to share the same buckling patterns; nevertheless, we consider only three dimers for simplicity.
- ⁴⁹In Ref. 17, it is reported that the RS structure was found by structure optimization using the initial structure generated by adding a Ge dimer to the most stable PD structure.
- ⁵⁰Y. Yoshimoto, Y. Nakamura, H. Kawai, M. Tsukada, and M. Nakayama, *Phys. Rev. B* **61**, 1965 (2000).
- ⁵¹C. Filippi, D. J. Singh, and C. J. Umrigar, *Phys. Rev. B* **50**, 14947 (1994).
- ⁵²S. Q. Wang and H. Q. Ye, *J. Phys.: Condens. Matter* **15**, L197 (2003).
- ⁵³D. Alfè and M. J. Gillan, *J. Phys.: Condens. Matter* **18**, L435 (2006).
- ⁵⁴D. Yu and M. Scheffler, *Phys. Rev. B* **70**, 155417 (2004).
- ⁵⁵A. E. Mattsson and D. R. Jennison, *Surf. Sci. Lett.* **520**, L611 (2002).